Oxygen-concentration dependence of the Raman continua in $YBa_2Cu_3O_y$ single crystals

X. K. Chen, E. Altendorf, and J. C. Irwin
Department of Physics, Simon Fraser University, Burnaby, British Columbia, Canada V5A 1S6

R. Liang and W. N. Hardy
Department of Physics, University of British Columbia, Vancouver, British Columbia, Canada V6T 1Z1
(Received 21 May 1993)

The low-energy portion ($\omega \leq 1200$ cm^{-1}) of the electronic Raman-scattering continua of $YBa_2Cu_3O_y$ single crystals with $y = 7.0$, 6.99, and 6.93 has been investigated in a temperature range from 20 to 100 K. The frequency distribution of the B_{1g} electronic continuum has been observed to be very sensitive to oxygen concentration. In particular a broad peak in the continuum shifts from 470 cm^{-1} to 550 cm^{-1} as y is reduced from 7.0 to 6.93. In contrast, the spectral distribution of the A_{1g} continuum is essentially the same for all three crystals with $y \geq 6.93$. The dependence of the continua on oxygen concentration is compared to the results of previous measurements of the phonon anomalies associated with the Raman-active c-axis oxygen vibrations in $YBa_2Cu_3O_y$. A symmetry-allowed correlation is established between the electronic continua and the phonon anomalies. Although the origin of the Raman continua remains undetermined, various possibilities are discussed and it is suggested that the B_{1g} continuum arises at least in part from scattering from spin-density fluctuations.

INTRODUCTION

Many Raman-scattering[1] and infrared-reflectivity[2] experiments have been carried out in an attempt to gain insight into the pairing mechanism and the nature of the superconducting gap in high-temperature superconductors. A significant number of the Raman experiments[3–11] have probed the low-energy ($\omega < 1000$ cm^{-1}) portion of the electronic continuum scattering that appears[12] to be present in all cuprate hole superconductors. It is found that as the sample temperature T is reduced below the critical temperature T_c the approximately flat ($T > T_c$) continuum redistributes into broad peaks which might be interpreted[5,6,9] as a measure of the superconducting gap, 2Δ. The straightforward identification of these peaks with 2Δ is, however, clouded because of the unknown origin of the continua which extend to very high frequencies ($\omega \geq 8000$ cm^{-1}), the scattering which is usually present[5,6,10] at frequencies less than 2Δ in the superconducting state, and because of the unusual temperature and doping dependence[8–11] of the peak frequencies. Infrared reflectivity spectra have also failed to produce a definitive picture of the gap.[2]

Recently, another group of experiments, both Raman[13–18] and far-infrared reflectivity (FIR),[19] has attempted to obtain information on the gap from comparisons of the superconductivity-induced (SCI) changes in the phonon frequencies ($\Delta\omega_v$) and linewidths ($\Delta\gamma_v$) with the predictions of a strong-coupling model (ZZ model).[20] These experiments have been primarily focused on $YBa_2Cu_3O_y$ (Y 1:2:3), in which the c-axis vibrations exhibit significant changes in ω_v and γ_v when T is reduced below T_c. In Raman experiments, the 340 cm^{-1} phonon, which has approximate B_{1g} symmetry[21] and arises from out of phase vibrations[1] of the planar oxygen atoms, shows particularly large effects[13,14] and this mode has been central to obtaining gap estimates in Y 1:2:3. In a determination of a gap energy from phonon renormalization measurements the Stuttgart group[13,14] obtained evidence for a single, sharp gap at $2\Delta \approx 320$ cm^{-1} in Y 1:2:3 and substituted variants all of which had $T_c \approx 90$ K. Subsequent Raman experiments,[15–18] however, demonstrated that the value of 2Δ obtained in this manner[14] was very sample dependent, in contrast to the results of continuum measurements. For example B_{1g} phonon renormalization measurements[17] yielded a value of $2\Delta = 340 \pm 20$ cm^{-1} in a fully oxygenated ($y = 7.0$) Y 1:2:3 crystal, but 2Δ increased to 360 ± 20 cm^{-1} when y was reduced to 6.99 and to 400 ± 20 cm^{-1} in a crystal with $y = 6.93$, despite the fact that T_c increased by only 4 K in the same concentration interval. Also some experiments[15,18] have found that the behavior of the A_g oxygen vibrations at 440 and 500 cm^{-1} is inconsistent with a gap value determined by the B_{1g} phonon renormalization and it has been suggested[18] that modes of different symmetry couple to different electronic excitations. Thus the phonon renormalization measurements imply that Y 1:2:3 may be characterized by an anisotropic gap and not by a single value for 2Δ. More generally, values of 2Δ extracted from phonon renormalization measurements must be received with skepticism because of the unknown origin of the phonon anomalies.

In the above experiments it is assumed that one is measuring excitations across a superconducting gap, and that the phonon anomalies are superconductivity induced. If this assumption is realized one must conclude from the doping dependence of 2Δ values obtained that the density of states near the Fermi surface depends very sensitively[17] on oxygen concentration. In an attempt to measure this dependence directly and hopefully clarify the ambiguities present in the phonon renormalization

measurements, we have carried out an investigation of the electronic Raman continua in samples with oxygen concentrations in the interval $6.93 \leq y \leq 7.0$. The results of the measurements clearly indicate that the B_{1g} phonon anomaly arises from interactions with the B_{1g} continuum and further suggest that the A_g phonons are coupled to the A_{1g} continuum. A symmetry-allowed correlation is then established between the electronic continua and the phonon renormalization measurements. However, we will also argue that the doping dependence of the continua might be more easily explained if it is assumed that the B_{1g} continuum arises at least in part from spin-density fluctuations and the B_{1g} phonon anomalies arise when a pseudogap develops[21] in the spin spectrum, at a temperature $T \gtrsim T_c$.

EXPERIMENT AND DATA ANALYSIS

The Raman spectra were obtained in quasibackscattering geometry using the 514.5 nm line of an Argon ion laser with an incident intensity ≤ 10 W/cm^2. The low power levels were used to minimize local heating of the sample by the laser, but in spite of this precaution it is possible[8] that the excited region of the crystal was heated by $\Delta T \leq 10$–20 K. The incident light was polarized along x' (1,1,0) and the scattered light along either x' or y' (1,−1,0). Considered within the tetragonal point group these geometries allow coupling to either the $A_{1g}(x'x')$ or $B_{1g}(x'y')$ continuum. The crystals used in this work were grown by a flux method in *YSZ* crucibles as described in detail elsewhere.[22] The annealing conditions used to obtain the crystals with different oxygen content have also been described previously[17] as have the methods and results of experiments used to characterize the crystals. Briefly, the oxygen content was estimated from the thermodynamic parameters[23] used in the annealing process and a refined estimate was then obtained[18] from the measured c-axis lattice parameters. The absolute value of the oxygen concentration thus obtained for each crystal may be somewhat less ($\lesssim 0.03$) than the quoted values but the relative values are fixed by the measured c-axis parameters. This paper will discuss results obtained on three different high-quality[17,18,22] crystals whose properties are summarized in Table I.

The A_{1g} spectra obtained from each crystal at an ambient temperature of 20 K are shown in Fig. 1. These spectra are similar in nature to those obtained previously[4,5] from fully oxygenated $T_c \sim 91$ K crystals. From Fig. 1 it is evident that there is very little variation in the continuum portion of the spectra with oxygen content. In

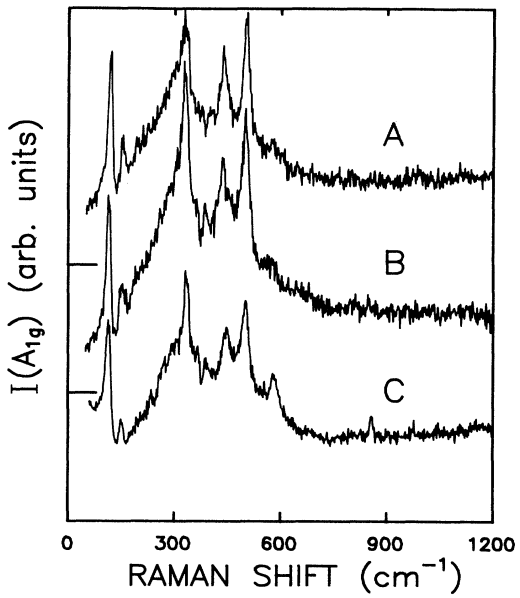

FIG. 1. Spectra obtained from crystals A, B, and C (see Table I) at 20 K in the $A_{1g}(x'x')$ scattering geometry.

Fig. 2, the B_{1g} spectra, obtained at 20 K from the same three crystals, are presented. This shows quite clearly, in contrast to the A_{1g} spectra, that there are significant changes in the B_{1g} continua as the oxygen concentration of the sample is varied. For example, if one uses the 500 cm^{-1} photon as a reference, it is evident that the broad peak in the continuum shifts to higher energies as y is decreased. In addition this peak is more clearly defined in samples A and B than it is in sample C. That is, the slope on the low-energy side of the maximum is steeper for A and B than in C and in addition this slope is greater than the slope at low energies ($\omega < 250$ cm^{-1}).

In order to focus more clearly on these continuum features we have attempted to remove the phonons from the spectra. The Raman scattering cross section for electronic scattering can be shown[24] to be proportional to the imaginary part of the Raman-scattering response function $\rho(\omega)$ multiplied by a thermal factor $[1+n(\omega,T)]$ where $n(\omega,T)=[\exp(\hbar\omega/k_BT)-1]^{-1}$. Figure 3 shows $\rho(\omega)$ obtained in the $A_{1g}(x'x')$ geometry at four temperatures for each of the three crystals. The spectra shown in Fig. 3 where obtained by dividing the original spectra by $[1+n(\omega,T)]$ and subtracting off the phonons. This was a relatively straightforward procedure for most of

TABLE I. c-axis lattice parameters (c_0), oxygen concentrations (y), results of magnetic measurements [T_c and ΔT_c (10–90 %)], and the peak frequencies (± 10 cm^{-1}) of continua at 20 K taken from Figs. 3 and 6.

Crystal	c_0 (Å)	y	T_c (K)	ΔT_c (K)	Peak frequencies (20 K) $A_{1g}(x'x')$	$B_{1g}(x'y')$
A	11.688	7.0	89.7	2.5	310	470
B	11.689	6.99	92.8	0.8	310	490
C	11.698	6.93	93.7	0.2	310	550

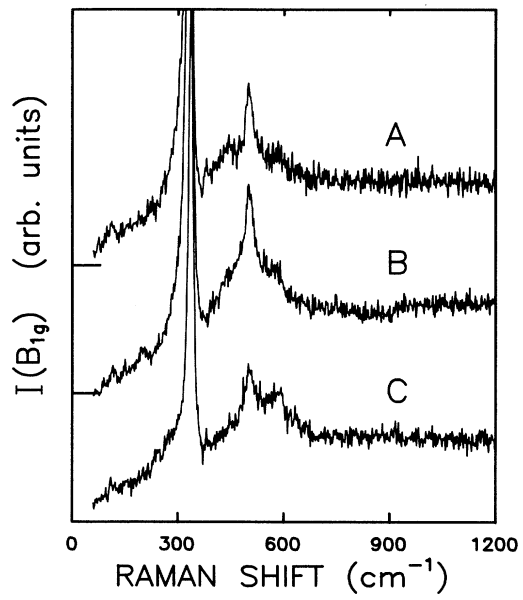

FIG. 2. Spectra obtained from crystals A, B, and C (see Table I) at 20 K in the $B_{1g}(x'y')$ scattering geometry.

the phonons since they are either quite symmetric, or quite weak, or both. In these cases, a portion of the spectrum covering a phonon line was fitted to a Lorentzian (or Fano) profile plus a background described by a polynomial up to the second order. Then the fitting parameters were used to generate a phonon profile over a wider frequency range and this profile was then subtracted from the spectrum. It should be noted that the measured phonon linewidths used in this work were not corrected for instrumental broadening since, as will be described shortly, we were able to obtain good fits to the as-measured spectra and the broadening introduced by our spectrometer is small compared to the broad feature of the continua, in which we are interested.

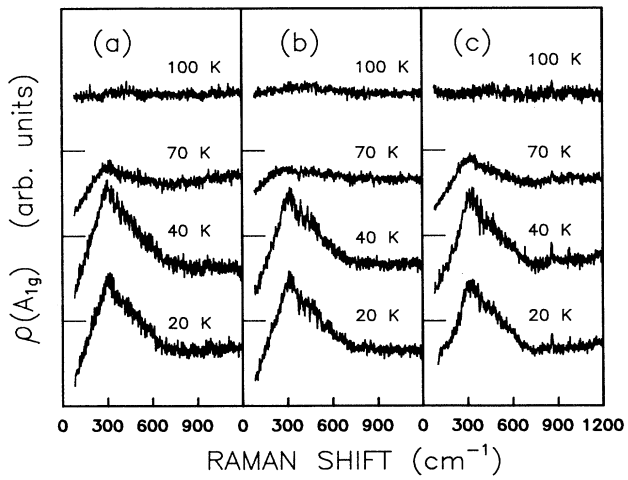

FIG. 3. Imaginary part $\rho(\omega)$ of the response function, with phonons subtracted, acquired in the $A_{1g}(x'x')$ scattering geometry for (a) crystal A ($y=7.0$); (b) crystal B ($y=6.99$), and (c) crystal C ($y=6.93$) at the temperatures indicated. The zero-intensity levels are indicated by the short lines inserted on the vertical axis. All spectra are plotted with the continua ($\omega \approx 800$ cm^{-1}) normalized to unity.

A simple subtraction procedure is inappropriate for removal of the 340 cm^{-1} B_{1g} phonon as it is both very asymmetric and very intense and the interaction between the phonon and the continuum considerably affects the shape of the spectrum. The continuum must be extracted from the spectrum through a more detailed decoupling procedure. To proceed we will adopt a formalism similar to that described by Klein.[25] As shown in Fig. 4, the system has a ground state $|g\rangle$, a phonon excited state $|p\rangle$, and a continuous distribution of the electronic states $|e_i\rangle$ ($i=1,2,\ldots$). The Raman matrix elements associated with the transitions from the ground state to states $|p\rangle$ and $|e_i\rangle$ are T_p and T_e. The perturbation of electron-phonon coupling is assumed to be present in the form of a matrix element V between $|p\rangle$ and $|e_i\rangle$. For simplicity we assume V, T_p, and T_e are real, and V and T_e are independent of frequency.

Following Klein's approach,[25,26] the Green's function operator can be written as

$$G(\omega)=\begin{bmatrix} g_p^{-1}(\omega) & V \\ V & g_e^{-1}(\omega) \end{bmatrix}^{-1} . \tag{1}$$

The unperturbed Green's functions for the phonon $g_p(\omega)$ and the electronic continuum $g_e(\omega)$ can be written as

$$g_p(\omega)=\frac{1}{\omega_p-\omega-i\Gamma} , \tag{2}$$

$$g_e(\omega)=-R(\omega)+i\rho(\omega) , \tag{3}$$

where the real and imaginary part of the electronic response function, $R(\omega)$ and $\rho(\omega)$, are related by the Kramers-Kronig relations. The unperturbed Raman line of the phonon is assumed to be a Lorentzian with frequency ω_p and linewidth Γ. This in effect assumes that the phonon is homogeneously broadened, an assumption that appears to be justified in that the phonon frequency and linewidth are independent of the position sampled in a given crystal. The coupled Raman spectrum is given by

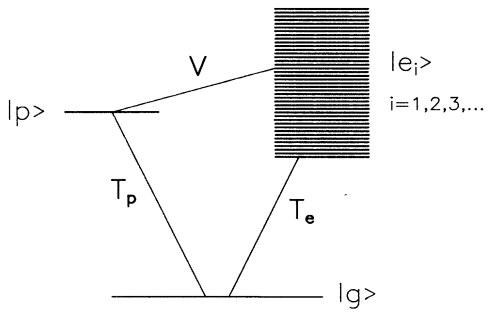

FIG. 4. Schematic diagram of the energy levels involved in the electron-phonon interaction process (Ref. 25).

$$I(\omega)=A[1+n(\omega)]\mathrm{Im}[\chi(\omega)]\ , \tag{4}$$

where

$$\chi(\omega)=T_p^2G_{11}+T_pT_eG_{12}+T_eT_pG_{21}+T_e^2G_{22} \tag{5}$$

is the dielectric susceptibility. It is straightforward to work out the matrix inversion, and (4) becomes

$$I(\omega)=A[1+n(\omega)]\mathrm{Im}\left[\frac{T_p^2g_e^{-1}-2VT_pT_e+T_e^2g_p^{-1}}{g_e^{-1}g_p^{-1}-V^2}\right]$$
$$=B[1+n(\omega)]\left[\rho(\omega)+\frac{1}{\gamma(1+\varepsilon)}\left[\frac{S^2}{V^2}+2\rho(\omega)\varepsilon S-\rho^2(\omega)V^2\right]\right]\ , \tag{6}$$

where γ, ε, and S are defined as

$$\gamma=\Gamma+V^2\rho(\omega)\ ,$$
$$\varepsilon=(\omega-\omega_v)/\gamma\ ,$$
$$S=V\frac{T_p}{T_e}+V^2R(\omega)\ ,$$

where $B=AT_e^2$ and $\omega_v=\omega_p+V^2R(\omega)$.

In Eq. (6), the first term represents the pure electronic continuum arising from the imaginary part of the electronic response function, the second term basically gives the phonon contribution,[27] and the last two terms result from the coupling effects. In the Raman spectrum, the contribution from the real part of the electronic response function $R(\omega)$ should be small since that contribution is only due to the electron-phonon coupling V which is considered as a perturbation. Moreover, it can be seen from Eq. (6) that the contribution of $R(\omega)$ decreases as $|\omega-\omega_v|\approx|\omega-\omega_p|$ becomes large. In other words, the contribution of the real part of the electronic response function is small and is confined to a relatively small frequency region near the phonon. Since we are mainly interested in the unperturbed electronic continuum arising from the imaginary part of the electronic response function, rather than the details of the real part, we will treat the latter as frequency independent, that is, both S and ω_v will be considered as frequency independent.

A B_{1g} spectrum with the 340 cm^{-1} phonon present was fitted to Eq. (6) by a nonlinear least-squares-fit procedure, in which B, Γ, ω_v, S, and V were treated as fitting parameters, and the imaginary part of the electronic response function $\rho(\omega)$ was described by a smooth function obtained by a fourth-order spline fit (see the dashed line in the inset of Fig. 5). More specifically, the parameters B, Γ, ω_v, S, and V were first determined by fitting the spectrum in the frequency range of 50 $\mathrm{cm}^{-1}\le\omega\le650$ cm^{-1} with $\rho(\omega)$ described by a sixth-order polynomial. Then, $\rho(\omega)$ in the whole frequency range (50 $\mathrm{cm}^{-1}\le\omega\le1200$ cm^{-1}) was obtained by subtracting the last three terms of Eq. (6) from the spectrum (and dividing by $B[1+n(\omega,T)]$), and smoothed by using a fourth-order spline fit. The result for $\rho(\omega)$ was refined by repeated iterations in which a term proportional to the difference between the data and the spectrum generated from Eq. (6) was used as the iterating correction for $\rho(\omega)$. An example illustrating the quality of the fits that were obtained is shown in Fig. 5. In other words, for each spectrum, we have found the values of a set of five parameters B, Γ, ω_v, S, and V, and a numerically determined smooth function $\rho(\omega)$, which can be substituted into Eq. (6) to generate a Raman spectrum which is in excellent agreement with the experimental data in the frequency range 50 $\mathrm{cm}^{-1}\le\omega\le1200$ cm^{-1}. The values of the fitting

TABLE II. Fitting results of B, Γ, ω_v, S, and V.

Crystal	T (K)	B (arb. unit)	Γ (cm^{-1})	ω_v (cm^{-1})	S (cm^{-1})	V (cm^{-1})
	20	0.240	8.97	332.8	−11.5	0.71
A	40	0.122	9.88	332.9	−9.47	0.51
	70	0.099	11.2	340.9	−5.21	0.43
	100	0.065	8.91	341.1	−3.25	0.21
	20	0.481	7.40	335.0	−9.43	0.82
B	40	0.241	7.62	335.0	−11.3	0.69
	70	0.066	8.52	342.0	−7.02	0.35
	100	0.023	7.99	343.1	−7.15	0.18
	20	0.089	6.59	338.6	−6.52	0.27
C	40	0.091	7.23	340.6	−6.34	0.29
	70	0.029	7.51	340.4	−5.10	0.17
	100	0.013	8.13	343.8	−5.25	0.13

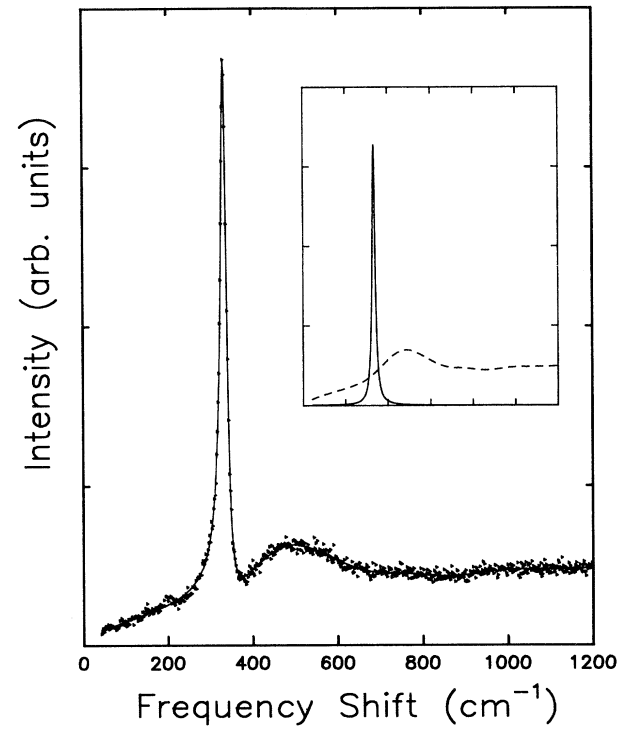

FIG. 5. Fitting of the B_{1g} spectrum ($y=6.99$, $T=20$ K). The triangles represent the data points and the solid line is generated from Eq. (6), and the spectra have been divided by the Bose-Einstein thermal factor. The solid line in the inset represents the S^2 term in Eq. (6) which is essentially the phonon contribution. The dashed line in the inset is the fitting result of the pure electronic continuum.

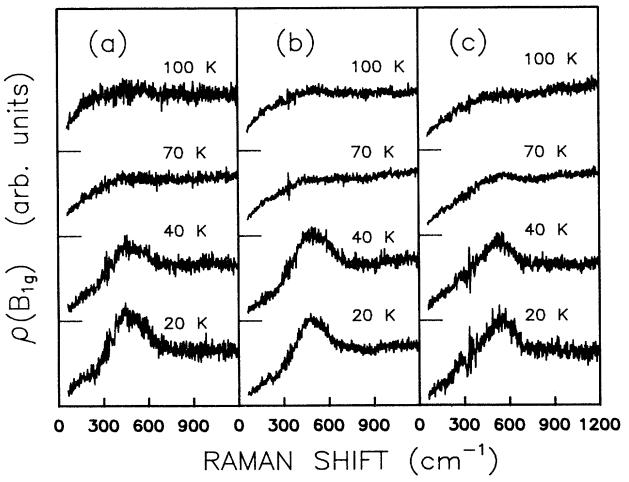

FIG. 6. B_{1g} electronic continuum with the phonons removed: (a) crystal A ($y=7.0$); (b) crystal B ($y=6.99$), and (c) crystal C ($y=6.93$) at the temperatures indicated. The zero-intensity levels are indicated by the short lines inserted on the vertical axis. All spectra are plotted with the continua ($\omega\approx 800$ cm^{-1}) normalized to unity.

parameters B, Γ, ω_v, S, and V for the spectra shown in Fig. 6 are listed in Table II. It should be noted that previous[14,17,18] fitting procedures used a linear background term in addition to the Fano profile, but with the present model [Eq. (6)] excellent agreement is obtained without the incorporation of such a background term.

RESULTS AND DISCUSSION

Examination of the A_{1g} spectra in Fig. 3 reveals that the peak frequency at 20 K is the same (310 ± 10 cm^{-1}) for all three crystals and is thus independent of oxygen concentration. The spectral distribution of the continua is also quite similar for all three crystals although the scattering intensity at low frequencies ($\omega<150$ cm^{-1}) appears to be greater in crystal C than it is in crystals A and B. If the relatively flat portions of the continua ($\omega>700$ cm^{-1}), which are normalized to unity in Fig. 3, are extrapolated to lower frequencies to provide a base line, the area above the base lines is the same for all three samples to within the estimated uncertainty ($\approx\pm15\%$). The observed temperature dependence of both the peak frequencies and the areas above the base lines is in good agreement with previous results[7] in Y 1:2:3. For our purposes the most significant aspect of the above results is that the peak position and the frequency distribution of the A_{1g} continuum are relatively independent of oxygen concentration for $6.93<y<7.0$. This result can be compared to the observation[18] that the measured phonon anomalies for the A_g phonons were also approximately the same for crystals A, B, and C. In this regard, however, one should note that the A_g phonon renormalization measurements were carried out[18] in a (zz) geometry while the present measurements of the A_{1g} continua were obtained with polarizations in the ab plane. Our preliminary measurements on the above crystals and previous results,[16] however, both suggest that $\Delta\gamma_v$ and $\Delta\omega_v$ for the A_g phonons are approximately independent of the scattering geometry. A coupling of the A_g phonons to the A_{1g} continuum is thus consistent with the above results.

The B_{1g} continua with the phonons removed are shown in Fig. 6. In this geometry the normalized area above the base line, defined as above, appears to decrease by about 25% (for $T=20$ K) as the oxygen content is decreased from $y=7.0$ (crystal A) to $y=6.93$ (crystal C), but again this value is comparable to our experimental uncertainty and no definitive conclusion is reached. However, the most interesting aspect of the B_{1g} spectra at 20 K is that the peak frequency of the broad maximum shifts from about 470 cm^{-1} in the continuum obtained from crystal A to about 550 cm^{-1} in the continuum obtained from crystal C. This 80 ± 20 cm^{-1} shift is comparable to the increase (60 ± 20 cm^{-1}) in 2Δ between crystals A and C that was predicted from the comparison[14] of the phonon renormalization measurements with the ZZ model. The B_{1g} continua at 20 K for crystals A, B, and C are replotted in Fig. 7 to more clearly illustrate the shift of peak frequency as a function of y. It is also interesting to extrapolate the base line, defined by the higher-energy (700 cm$^{-1}<\omega<1100$ cm^{-1}) portion of the continuum, to intercept the lower-energy portion as indi-

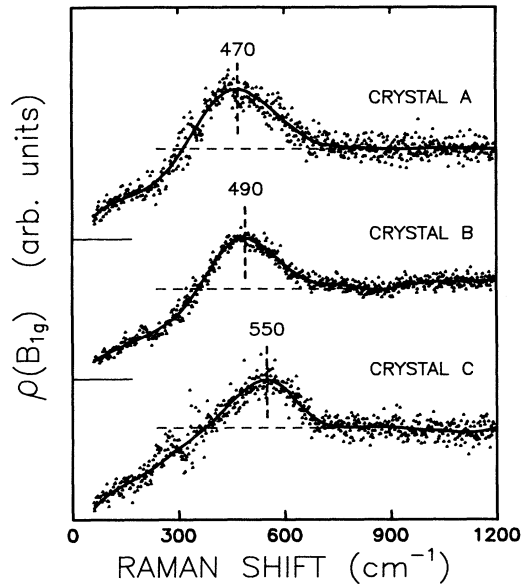

FIG. 7. B_{1g} continua at 20 K for crystals A, B, and C as obtained from the fitting procedure described in the text.

cated by the horizontal dashed lines in Fig. 7. The intercept of these lines with the continua should approximately defined the frequencies below which spectral weight is removed and above which spectral weight is added. In this case the interception points occur at about 330 cm^{-1} for crystal A, 360 cm^{-1} for crystal B, and 390 cm^{-1} for crystal C. These values are in almost exact agreement with the superconducting "gap" energies obtained from comparisons[17] of the phonon renormalization measurements with the strong-coupling model. This agreement strongly suggests that the gap energy determined from the phonon renormalization measurements is in fact the "crossover" energy of the B_{1g} continuum.

From Fig. 6 it can be seen that there is a clear change of slope of the continuum near 250 cm^{-1}, yielding a frequency distribution that is suggestive of the initial stage of the development of a "clean" gap similar to that observed[10,11] in Bi 2:2:1:2. Staufer *et al.*[10] found that evidence of such a "clean" gap in the B_{1g} continuum was obtained in an overdoped crystal of Bi 2:2:1:2, and that this gap became partially filled in by scattering at $\omega < 2\Delta$ in a crystal with lower oxygen content. The doping dependence observed here for Y 1:2:3 appears to follow the same trend in that we observed additional scattering at low frequencies for crystal C and as a result the above gap feature is not as clearly defined in crystal C. Thus the B_{1g} continuum represents another aspect of the electronic scattering that suggests a common origin,[10] namely the Cu-O planes, for the major features of the continua in the two compounds.

The above results demonstrate quite convincingly that the observed renormalization of the B_{1g} phonon near T_c arises from interactions with those excitations that are responsible for the B_{1g} continuum. The origin of the B_{1g} continuum, however, remains unclear. It has been suggested[28] that the B_{1g} continuum arises from interband transitions. The sensitivity of the spectral distribution of the continua to oxygen concentration could result if, for example, these bands were associated with the Cu(1)-O(1) chains, but a fortuitous set of circumstances would then be required to explain the low-energy redistribution of the states associated with the onset of superconductivity.

An alternative approach is to assume the continua arise from excitations which participate in the formation of a superconducting gap or gaps.[5,9,10] The *ZZ* model[20] can thus be used to predict the SCI shifts in frequency and linewidth, and comparisons[17] with experiment provide a value of 2Δ for each crystal. Furthermore, the observed temperature dependence of the linewidth ($T < T_c$) is in good agreement[17,18] with the model[20] predictions. Finally, the dependence of 2Δ on y, as determined from the phonon measurements, is correlated with the y dependence of the B_{1g} continuum. This internal consistency could be interpreted as support for the applicability of the *ZZ* model[20] and as evidence that the B_{1g} continuum arises from electronic excitations across a portion of an anisotropic gap.[5] One would then have a speculate that, when y is reduced from 7.0 to 6.93, the magnitude of the gap in this region of the Fermi surface increases significantly (16%) while T_c increases by only 4%, as indicated by the above results. This scenario would appear to be at least plausible, if T_c is primarily associated with the gap in other regions of the Fermi surface.

As an alternative explanation for the B_{1g} spectrum and its doping dependence, let us speculate that it arises, if not totally, at least in part from spin-density fluctuations. There are previously published results[19,29,30] that appear to provide support for such a speculation. Based on the phenomenological Ginzburg-Landau theory developed by Nagaosa and Lee,[21] it can be shown that the spin pseudogap $\Delta_s \sim J|T - T_D|^{1/2}$ increases with decreasing oxygen concentration in Y 1:2:3 since the transition temperature T_D for the pairing of the spinons increases with decreasing hole doping.[21] Also, for the underdoped Y 1:2:3 crystals, that is, $T_D > T_c$. Experimentally Litvinchuk, Thomsen, and Cardona,[19] in FIR and Raman experiments on $YBa_2Cu_4O_8$ ($T_c = 78$ K) and Y 1:2:3 ($y = 6.57$) found phonon anomalies that occurred well above T_c and suggested that such anomalies result from a coupling of the phonons to the spin and the opening of a pseudogap at $T > T_c$. Given a correlation between the continua and phonon anomalies one might expect, in oxygen-reduced crystals, to see evidence for the formation of a pseudogap in the spectra at temperatures $T > T_c$. There is no such evidence in our data but this is perhaps not surprising in that we are working with doping levels relatively close to optimum.[21] However, Slakey *et al.*[29] observed that the peak in the B_{1g} continuum was established at temperatures well above T_c in a crystal with $y \approx 6.7$, $T_c \approx 60$ K. Also, in a recent FIR study of the *c*-axis reflectivity of an Y 1:2:3 crystal with $y = 6.7$ and $T_c = 63$ K Homes *et al.*[30] have attributed a reduction in the conductivity at low frequencies ($\omega < 200$ cm^{-1}) and temperatures ($T < 150$ K) to the formation of a pseudogap. In the present case we assume that the "gap" energy derived from the phonon re-

normalization measurements (and crossover energy of the B_{1g} continuum) will be close to 2Δ for doping levels near optimum and that as we move into the underdoped region we will obtain an estimate of the pseudogap energy which is larger in magnitude than the superconducting gap, in agreement with past[17,18] and present observations. Then, the sensitive dependence of the B_{1g} continuum on the oxygen concentration observed in the present work suggests that the magnitude of the spin pseudogap in Y 1:2:3 is very sensitive to the doping level.

CONCLUSIONS

In conclusion we have carried out Raman-scattering investigations of the electronic continua in differently doped Y 1:2:3 single crystals. At low temperature ($T=20$ K) the frequency distribution of the B_{1g} continuum is observed to vary significantly with small changes in the oxygen concentration y while the A_{1g} spectrum is essentially independent of y for $y \geq 6.93$. Comparisons with measurements[17,18] of the renormalization of the Raman-active c-axis oxygen vibrations have been carried out and the results have established a symmetry-allowed correlation between the electronic continua[4,5] and the phonon anomalies observed[13–18] in Y 1:2:3. The doping dependence of the spectral distribution of the B_{1g} continua is qualitatively similar to that observed[10] in Bi 2:2:1:2, which suggests similar origins for the low-energy portions of the continua in the two compounds, in agreement with previous[10] conjectures. Finally, the exact nature of the excitations which give rise to the continua remains undetermined by this work. However, the doping dependence of the correlated phonon anomalies and continua, the conjunction with previous[19,29] measurements in underdoped systems, suggests that the B_{1g} continuum is at least in part due to interaction with spin-density fluctuations and that the formation of a spin pseudogap[21] is observed in underdoped samples.

ACKNOWLEDGMENTS

The authors would like to thank G. Soerensen, Dr. S. Gygax, Dr. J. Carolan, P. Dosanjh, W. Xing, and Dr. B. Heinrich for carrying out the magnetic measurements on the crystals and Dr. J. Dahn for his assistance in carrying out the x-ray measurements. The financial support of the Natural Sciences and Engineering Council of Canada is gratefully acknowledged.

[1] C. Thomsen, in *Light Scattering in Solids VI*, edited by M. Cardona and G. Güntherodt (Springer-Verlag, Berlin, 1991).
[2] D. B. Tanner and T. Timusk, in *Physical Properties of High Temperature Superconductors III*, edited by D. M. Ginsberg (World Scientific, Singapore, 1992).
[3] For a brief review see Ref. 1.
[4] S. L. Cooper, M. V. Klein, B. G. Pazol, J. P. Rice, and D. M. Ginsberg, Phys. Rev. B **37**, 5920 (1988).
[5] S. L. Cooper, F. Slakey, M. V. Klein, J. P. Rice, E. D. Bukowski, and D. M. Ginsberg, Phys. Rev. B **38**, 11 934 (1988).
[6] R. Hackl, W. Gläser, P. Müller, D. Einzel, and K. Andres, Phys. Rev. B **38**, 7133 (1988).
[7] R. Hackl, P. Müller, D. Einzel, and W. Gläser, Physica C **162-164**, 1241 (1989).
[8] A. A. Maksimov, A. V. Puchkov, and I. I. Tartakovskii, Solid State Commun. **81**, 407 (1992).
[9] M. Boekholt, M. Hoffmann, and G. Güntherodt, Physica C **175**, 127 (1991).
[10] T. Staufer, R. Newetchek, R. Hackle, P. Müller, and H. Veith, Phys. Rev. Lett. **68**, 1069 (1992).
[11] M. Boekholt, G. Gütherodt, and A. Moshchalkov, Physica C **192**, 191 (1992).
[12] S. Sugai, Y. Enomoto, and T. Murakami, Solid State Commun. **75**, 975 (1990).
[13] C. Thomsen, M. Cardona, B. Friedl, C. O. Rodriguez, I. I. Mazin, and O. K. Andersen, Solid State Commun. **75**, 219 (1990).
[14] B. Friedl, C. Thomsen, and M. Cardona, Phys. Rev. Lett. **65**, 915 (1990).
[15] K. F. McCarty, H. B. Radousky, J. Z. Liu, and R. N. Shelton, Phys. Rev. B **43**, 13 751 (1991).
[16] E. Altendorf, J. Chrzanowski, J. C. Irwin, A. O'Reilly, and W. N. Hardy, Physica C **175**, 47 (1991).
[17] E. Altendorf, J. C. Irwin, R. Liang, and W. N. Hardy, Phys. Rev. B **45**, 7551 (1992).
[18] E. Altendorf, X. K. Chen, J. C. Irwin, R. Liang, and W. N. Hardy, Phys. Rev. B **47**, 8140 (1993).
[19] A. P. Litvinchuk, C. Thomsen, and M. Cardona, Solid State Commun. **83**, 343 (1992), and references therein.
[20] R. Zeyher and G. Zwicknagl, Z. Phys. B **78**, 175 (1990).
[21] N. Nagaosa and P. A. Lee, Phys. B **45**, 966 (1992); P. A. Lee and N. Nagaosa, *ibid.* **46**, 5621 (1992).
[22] R. Liang, P. Dosanjh, D. A. Bonn, D. J. Baar, J. F. Carolan, and W. N. Hardy, Physica C **195**, 51 (1992).
[23] P. Schleger, W. N. Hardy, and B. X. Yang, Physica C **176**, 261 (1991).
[24] M. V. Klein, in *Light Scattering in Solids I*, edited by M. Cardona (Springer-Verlag, Heidelberg, 1983).
[25] M. V. Klein, in *Light Scattering in Solids*, edited by M. Cardona (Springer-Verlag, Heidelberg, 1975).
[26] A. Nitzan, Mol. Phys. **27**, 65 (1974).
[27] B. Friedl, C. Thomsen, H.-U. Habermeier, and M. Cardona, Solid State Commun. **78**, 291 (1991).
[28] H. Monien and A. Zawadowski, Phys. Rev. Lett. **63**, 911 (1989).
[29] F. Slakey, M. V. Klein, J. P. Rice, and D. M. Ginsberg, Phys. Rev. B **42**, 2643 (1990).
[30] C. C. Homes, T. Timusk, R. Liang, D. A. Bonm, and W. N. Hardy, Phys. Rev. Lett. (to be published).